

CSR IMPEDANCE FOR AN ULTRARELATIVISTIC BEAM MOVING IN A CURVED TRAJECTORY

D. Zhou*, K. Ohmi and K. Oide, KEK/SOKENDAI, 1-1 Oho, Tsukuba, Ibaraki 305-0801, Japan

Abstract

A dedicated computer code, CSRZ, has been developed to calculate the coherent synchrotron radiation (CSR) impedance for an ultrarelativistic beam moving in a curved trajectory. Following the pioneering work of T. Agoh and K. Yokoya [1], the code solves the parabolic equation in the frequency domain in a curvilinear coordinate system. The beam is assumed to move along a vacuum chamber which has a uniform rectangular cross section but with variable bending radius. Using this code, we did investigations in calculating the longitudinal CSR impedance of a single and a series of bending magnets. The calculation results indicate that the shielding effect due to outer chamber wall can be well explained by a simple optical approximation model at high frequencies. The CSR fields reflected by the outer wall may interfere with each other in a long bending magnet and lead to sharp narrow peaks in the CSR impedance.

INTRODUCTION

CSR has been studied extensively in the literature (for instances, see Refs. [2]-[9]). We follow Agoh and Yokoya's method [1] to calculate CSR generated by a beam moving along an arbitrary trajectory inside a curved vacuum chamber. The trajectory can be generated by a single bending magnet (see Fig. 1), or a series of bending magnets. The relevant chamber along a series of bending magnets can be extended from Fig. 1. At present, we assume the chamber has a uniform rectangular cross-section along the beam trajectory. To close the problem, two long straight sections are added before the entrance and after the exit of the chamber. Meanwhile, the walls of the chamber are perfectly conducting and always parallel to the beam trajectory.

We continue the work presented in [1, 9] and do investigations in the follow aspects: 1) the features of longitudinal CSR impedance in a single bending magnet; 2) Optical approximation of CSR; 3) the interference of CSR fields in a series of bending magnets and its effects on the longitudinal impedance. This paper focuses on 1) and 2). The aspect of 3) was discussed in another independent paper (see Ref. [10]).

PROBLEM STATEMENT

The fundamental equation adopted in our studies of CSR is the parabolic equation in the frequency domain in a curvilinear coordinate with the origin on the beam trajec-

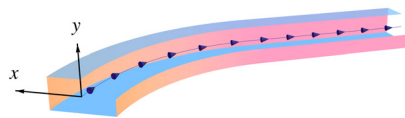


Figure 1: The geometry of the curved chamber for a single bending magnet. A infinitely long straight chamber is connected after the exit of the curved chamber. The beam moves along the curved line with arrows. The origin of the coordinate system coincides with the beam orbit.

tory [1, 11]

$$\frac{\partial \vec{E}_{\perp}}{\partial s} = \frac{i}{2k} \left(\nabla_{\perp}^2 \vec{E}_{\perp} - \frac{1}{\epsilon_0} \nabla_{\perp} \rho_0 + \frac{2k^2 x}{R(s)} \vec{E}_{\perp} \right), \quad (1)$$

where \vec{E}_{\perp} is the transverse electric field, and $R(s)$ is the s -dependent bending radius along the beam orbit. ϵ_0 is the vacuum permittivity. The beam is assumed to be rigid, i.e. the beam charge density ρ_0 does not vary along s . Equation (1) also describes the field evolution in a straight chamber where the inverse bending radius is zero.

With paraxial approximation [1], the longitudinal electric field is a byproduct of the transverse fields and approximated as

$$E_s = \frac{i}{k} \left(\nabla_{\perp} \cdot \vec{E}_{\perp} - \mu_0 c J_s \right), \quad (2)$$

where μ_0 is the vacuum permeability, c is the speed of light in vacuum, and $J_s = \rho_0 c$ is the current density. The detailed derivation of the above equations can be found in Refs. [11, 1]. We will not discuss the validity of these equations either, because it has been well addressed in Refs. [9, 8].

In our calculations, the beam has a point charge form in the longitudinal direction and Gaussian distribution in the transverse directions. Then the longitudinal impedance is calculated by directly integrating E_s over s

$$Z_{\parallel}(k) = -\frac{1}{q} \int_0^{\infty} E_s(x_c, y_c) ds \quad (3)$$

where (x_c, y_c) denotes the center of the beam in the transverse x - y plane. The appearance of the minus sign in Eq. (3) is due to the convention of the beam instability formalism.

The numerical algorithms adopted in our work are adapted from the mesh methods originally presented in [1]. We start by dividing the rectangular domain $(0, a) \times (0, b)$

05 Beam Dynamics and Electromagnetic Fields

D06 Code Developments and Simulation Techniques

* dmzhou@post.kek.jp

in the x - y plane into an equidistant $M \times N$ mesh with step sizes $\Delta x = a/M$ and $\Delta y = b/N$ in the x and y directions, respectively. The grid is shown in the solid lines of Fig. 2. The outer chamber wall is on the right side. The numerical techniques will not be discussed in this paper. The readers are referred to [1, 12] for details.

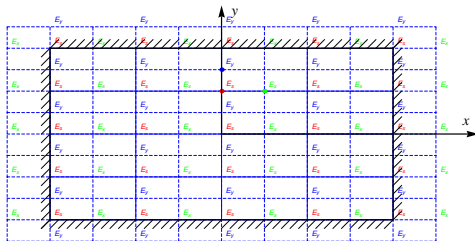


Figure 2: Staggered grid definition with ghost points outside the boundary of the chamber. The positions of various field components are shown. Constant spacing in the x and y directions is assumed.

NUMERICAL RESULTS FOR A SINGLE BENDING MAGNET

To calculate the longitudinal CSR impedance in a single bending magnet, the beam is assumed to move along the central line of the curved chamber, i.e. $x_c = a/2, y_c = b/2$. Investigations were performed to examine the influence of the magnet length on the longitudinal CSR impedance. For purpose of demonstration, we chose bending radius $R = 5$ m, chamber cross-section dimensions $a = 6$ cm and $b = 3$ cm. The magnet length is varied as $L_b = 0.5, 2, 8$ m. The impedance results are shown in Figs. 3(a) and 3(b). In the same figures, we also plot the results given by the parallel plates model in solid black lines [1]. And the corresponding wake potentials with a short bunch of rms length $\sigma_z = 0.5$ mm are given in Fig. 3(c). From the figures, one sees that when $L_b = 0.5$ m, which indicates a short curved chamber, the impedance is very smooth. When the curved chamber gets longer, the impedance becomes fluctuating with an interval of around 1.3 mm^{-1} in wavenumber and eventually results in a series of resonant peaks. This observation clearly indicates that the CSR impedance is actually related to the eigenmodes of the curved chamber [11]. When the curved chamber is long enough, some specific modes which fulfill the phase matching condition can be strongly excited by the beam and become dominant in the radiation field.

One can compare the wavenumbers at the resonant peaks in Fig. 3(a) with the analytical predictions which are available in Refs. [8, 5, 11]. According to [8], the resonance peaks should appear at wavenumbers of

$$k_{mn} = \frac{n\pi}{b} \sqrt{\frac{R}{x_b}} \Upsilon \left(\frac{b(m \pm 0.25)}{nx_b} \right), \quad (4)$$

where the integer indices m and n denote the individual mode of the curved chamber and x_b is the distance from

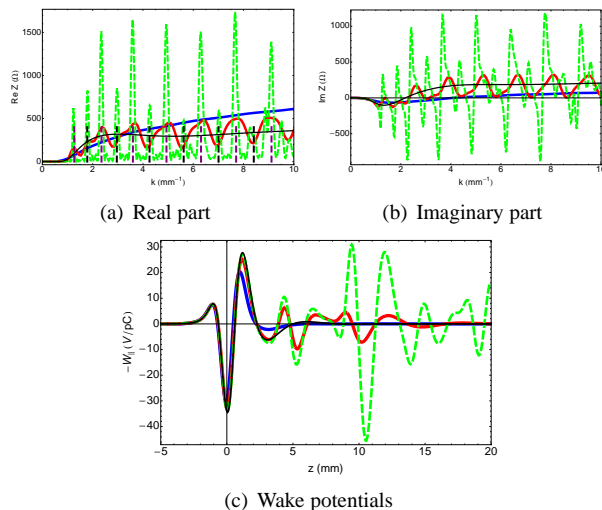


Figure 3: CSR impedance and wake potential for a single bending magnet. The impedances and wake potentials have been normalized by the length of the curved chamber. The purple and black dashed lines denote E_x and E_y modes with $n = 1$, respectively. Blue solid lines: $L_b = 0.5$ m; red solid lines: $L_b = 2$ m; green dashed lines: $L_b = 8$ m; black solid lines: parallel plates model.

the beam orbit to the outer wall in the horizontal plane. The plus sign in Eq. (4) indicates E_x modes in which $E_y = 0$ and $m = 0, 1, 2, 3, \dots$; the minus sign indicates E_y modes in which $E_x = 0$ and $m = 1, 2, 3, \dots$. According to [8], n must be odd and $n = 1, 3, 5, \dots$. Finally, $\Upsilon(r)$ is defined by

$$\Upsilon(r) = \left[\left(\sqrt{1 + \frac{r^2}{3}} + 1 \right)^{\frac{1}{3}} - \left(\sqrt{1 + \frac{r^2}{3}} - 1 \right)^{\frac{1}{3}} \right]^{-\frac{3}{2}}. \quad (5)$$

When r is large, $\Upsilon(r)$ can be approximated by $3r/2^{3/2}$ [8]. It implies that the resonance peaks in the CSR impedance are almost equally spaced along the wavenumber axis. The resonances are indicated by vertical dashed lines in Fig. 3(a). It turns out that they agree well with the observed peaks from numerical calculations.

OPTICAL APPROXIMATION OF OUTER-WALL REFLECTIONS

As stated in [8, 9], when the aspect ratio of the curved chamber a/b is larger than 2, the shielding of the inner and outer walls (walls on the left and right sides in Fig. 2) can be neglected and the parallel plates model is a good approximation for a long bending magnet. This criteria works well in the low frequency region with $k < k_{th}$ which was proved in [8]. Here k_{th} is the shielding threshold defined by [8]

$$k_{th} = \pi \sqrt{R/b^3}. \quad (6)$$

Our calculations do agree with this criteria. On the contrary, in the high frequency region, the CSR impedance

may significantly differs from the parallel plates model and exhibit fluctuations, even narrow resonance peaks for a long magnet. A geometrical explanation for this observation was proposed in Ref. [13] as illustrated in Fig. 4. The CSR field is radiated in the direction almost tangent to the beam trajectory when a beam enters the curved chamber. The outer wall plays a role of mirror and reflects the field back to the beam. If the curved chamber is long enough, the reflected fields can accumulate and interfere with each other. The geometrical picture of CSR suggests a critical length of

$$L_c = 2R\theta_c \approx 2\sqrt{2Rx_b}, \quad (7)$$

for the bending magnet. Here $\theta_c = \text{ArcCos}(R/(R+x_b)) \approx \sqrt{2x_b/R}$. If $L_b \gg L_c$, some specific modes can be strongly excited and results in the fluctuations or resonant peaks in the CSR impedance. If $L \leq L_c$, such fluctuations will be negligible. But if $L \ll L_c$, transient effect will also become important. The critical length indicates a length when the reflection of the outer wall becomes important. But L_c does not depends on the aspect ratio of the chamber cross-section. Therefore, the condition of neglecting outer-wall shielding, i.e. $L \leq L_c$, can be a supplement to the criteria of $a/b \geq 2$ which only applies at low frequency limit, i.e. $k < k_{th}$.

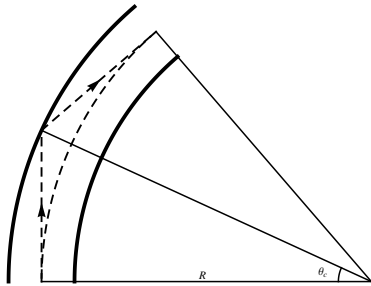


Figure 4: CSR reflected by the outer wall of the beam pipe. The beam starts to radiate fields at the entrance of the curved chamber. The dashed curve without arrows on it denotes the beam orbit. The arrowed dashed lines represent the direction of the radiation fields.

Similar to optical approximation in the theory of geometric impedance [14], the L_c defined by Eq. (7) can also be interpreted as a catch-up distance over which the CSR, generated by the head of a beam, reflects from the outer wall and reaches the beam tail at length Δs behind the head. It's easy to calculate Δs from the geometry shown in Fig. 4, and the result is [13]

$$\Delta s = 2R(\text{Tan}(\theta_c) - \theta_c) \approx \frac{4}{3}\sqrt{\frac{2x_b^3}{R}}. \quad (8)$$

The quantity Δs corresponds to a modulation frequency of [13]

$$\Delta k = \frac{2\pi}{\Delta s} \approx \frac{3\pi}{2}\sqrt{\frac{R}{2x_b^3}}. \quad (9)$$

It turns out that $\Delta k = k_{(m+1)n} - k_{mn}$ is exactly the distance between adjacent resonances for the same vertical index n and large argument r in Eq. (5). When comparing Δs with the bunch length σ_z , one can find another condition of neglecting outer-wall shielding effect in evaluating CSR induced instability, i.e. $\Delta s \gg \sigma_z$. Namely, this condition says that the reflected CSR fields from the outer wall can never catch up with the beam tail and thus has no influence on the beam in total.

One can check Eqs.(8) and (9) by applying them to the examples depicted in Fig. 3(a). $\Delta k = 1.4 \text{ mm}^{-1}$ is close to the observed value of 1.3 mm^{-1} . $\Delta s = 4.4 \text{ mm}^{-1}$ is roughly the distance at which the first peak appears in the tail part of the wake potential in Fig. 3(c). Since the bunch length $\sigma_z = 0.5 \text{ mm}$ is much smaller than Δs , the amplitude of the wake potential in the vicinity of the beam is almost independent of magnet length. Thus, one can conclude that the outer-wall shielding mainly impose effect in the tail part of CSR wake.

SUMMARY

In this paper we presented the numerical calculations of the longitudinal CSR impedance for a beam moving in a curved chamber. The CSRZ code was used to investigate the properties of CSR impedance of a single bending magnet. It turns out that the magnet length, in addition to the chamber aspect ratio, may also play an important role in defining the structure of CSR impedance. For a long magnet, the shielding effect of the outer wall can be well understood using an optical approximation model.

The author D.Z. would like to thank K. Yokoya, T. Agoh, G. Stupakov and Y. H. Chin for valuable discussions.

REFERENCES

- [1] T. Agoh and K. Yokoya, Phys. Rev. ST Accel. Beams, 7(5):054403 (2004).
- [2] B. G. Schinov, et al., Plasma Physics 15 (1973) 211.
- [3] A. Faltens and L. J. Laslett, Part. Accel. 4, 151. (1973).
- [4] K.-Y. Ng, Part. Accel. 25, 153. (1990).
- [5] R. L. Warnock and P. Morton, Part. Accel. 25, 113. (1990).
- [6] J. B. Murphy, et al., Part. Accel. 57, 9. (1997).
- [7] E. L. Saldin, et al., Nucl. Instrum. Methods A, 490:1-8, 2002.
- [8] T. Agoh, Phys. Rev. ST Accel. Beams, 12(9):094402 (2009).
- [9] G. V. Stupakov and I. A. Kotelnikov, Phys. Rev. ST Accel. Beams, 12(10):104401 (2009).
- [10] D. Zhou, et al., "Interference of CSR fields in a curved chamber", These proceedings.
- [11] G. V. Stupakov and I. A. Kotelnikov, Phys. Rev. ST Accel. Beams, 6(3):034401 (2003).
- [12] D. Zhou, PhD thesis, KEK/SOKENDAI, Sep. 2011.
- [13] K. Oide, Talk at CSR mini-workshop, KEK, Nov. 8, 2010.
- [14] G. V. Stupakov, et al., Phys. Rev. ST Accel. Beams, 10(5):054401 (2007).